

Bubble contributions to scalar correlators with mixed actions

Ziwen Fu¹

¹ *Key Laboratory for Radiation Physics and Technology of Education Ministry; Institute of Nuclear Science and Technology, College of Physical Science and Technology, Sichuan University, Chengdu 610064, People's Republic of China*

Within mixed-action chiral perturbation theory (MA χ PT), Sasa's derivation of the bubble contribution to scalar a_0 meson is extended to those of scalar κ and σ mesons. We revealed that κ bubble has two double poles and σ bubble contains a quadratic-in- t^2 growth factor stemming from the multiplication of two double poles for a general mass tuning of valence quarks and sea quarks. The corresponding preliminary analytical expressions in MA χ PT with $2 + 1$ chiral valence quarks and $2 + 1$ staggered sea quarks will be helpful for lattice studies of scalar mesons.

PACS numbers: 12.38.Gc, 11.15.Ha

I. INTRODUCTION

The nature of the lowest scalar meson is unveiled. Nowadays, σ meson was established with a low mass [1], and $a_0(980)$ meson is experimentally-confirmed, while κ meson is still disputable [1]. Moreover, there are long-lasting debates on the traits of the lowest scalar meson: is it a conventional $\bar{q}q$ or tetraquarks $\bar{q}\bar{q}qq$ [2–7]?

The tetraquark interpretation can easily realize the experimental mass ordering $m_{a_0(980)} > m_\kappa$ by lattice QCD, whereas the conventional $\bar{q}q$ states hardly explain this mass ordering [7–12]. Moreover, it is consistent with the MIT Bag Model [13]. Nevertheless, it is sharply criticized for overlooking some unresolved physical issues such as chiral symmetry breaking and non-trivial vacuum state [14], etc. This question can be partially reconciled if the masses of $\bar{q}q$ states with $I = 1/2, 1$ and 0 are robustly calculated on the lattice. We here call these states as κ , a_0 and σ mesons, respectively.

The a_0 meson was studied in staggered fermion [15, 16]. The propagators are discovered to hold the states with masses below the likely combinations of two physical mesons [15, 16], which can be nicely interpreted by the bubble contribution to the a_0 correlator (for simplicity, we call it “ a_0 bubble” in this work, likewise for “ κ bubble” and “ σ bubble”) derived by Sasa in MA χ PT [17].

We have been studying scalar meson for some time. With $2 + 1$ Asqtad-improved staggered sea quarks [18], we obtained κ mass: 826 ± 119 MeV [6], and rectified the taste-symmetry breaking by extending analyses of σ and a_0 mesons [17, 19–22] to κ meson in the staggered chiral perturbation theory (S χ PT) [23, 24]. We realized that κ bubble should be involved in a fit of κ correlator for the MILC medium coarse ($a \approx 0.15$ fm) and coarse ($a \approx 0.12$ fm) lattice ensembles. Moreover, bubble contributions to scalar correlators in S χ PT offers a test of lattice artifacts due to the fourth-root trick [17, 19].

Additionally, S χ PT predicts that these lattice artifacts vanish in the continuum limit, merely remaining physical thresholds [17, 19–24]. To check this prediction, we specially studied scalar mesons at a MILC fine ($a \approx 0.09$ fm) lattice ensemble [21, 24]. As expected, lattice artifacts are indeed significantly suppressed [21, 24].

Lattice studies with staggered fermions are cheaper than those of other fermion discretizations, which allow lattice studies with the smaller dynamical quark masses or finer lattice spacings. But, this benefits accompanies by an extra theoretical complications. Each staggered quark exists in four tastes [25], and staggered meson comes in sixteen tastes, and the taste symmetry breaking at $a \neq 0$ gives rise to discretization errors of $\mathcal{O}(a^2)$ [26]. Since these errors are usually not negligible, these unphysical effects predicted by S χ PT [26] should be neatly removed from the lattice data in order to extract the desired physical quantities.

Theoretically, lattice study with domain-wall (DW) quarks is simpler than that with staggered quarks since they do not come in multiple species [27, 28]. Consequently, it makes MA χ PT expressions for bubble contributions to scalar mesons simple and continuum-like [17, 30]. Moreover, they keep proper chiral symmetry up to exponentially small corrections at $a \neq 0$ [29]. Nonetheless, realistic simulations with DW fermions are expensive. We notice that there exists a pioneering study on a_0 meson with DW fermions [31].

MA χ PT for Ginsparg-Wilson type quarks on a staggered sea was proposed in Ref. [30]. Other quantities like a_0 bubble have since been added in MA χ PT [17, 32–35]. It is worth mentioning that only a couple of extra parameters enter the relevant chiral formulas. One of these parameters was determined by MILC Collaboration [16]. Aubin *et al* estimated another one inherent in the mixed-action case [31]. These parameters can be used to study other physical quantities: e.g., the bubble contributions to scalar mesons discussed in this work.

In this work we extend Sasa's original derivation on the bubble contribution to a_0 correlator [17] to those of κ and σ correlators in MA χ PT with $2 + 1$ chiral valence quarks and $2 + 1$ staggered sea quarks, and exploit two above-mentioned published parameters [16, 31] to elucidate our analytical expressions using two mass tuning. We found that κ and σ bubbles demonstrated many particular features, e.g., the strong infrared-sensitive unphysical effects due to the multiplication of two double pole to σ bubble. These analyses will be helpful for lattice determinations on scalar meson masses.

This paper is organized as follows. We review the necessary knowledge of MA χ PT in Sec. II, and deduce κ and σ bubbles in MA χ PT in Sec. III. We illustrate the obtained analytical expressions in Sec. IV. The conclusions are arrived in Sec. V. The corresponding S χ PT κ and σ bubbles are courteously dedicated to the Appendix.

II. MIXED ACTION χ PT

At leading-order quark mass expansion, the mixed action chiral Lagrangian is described by N_V Ginsparg-Wilson valence quarks and N_S staggered sea quarks [30]. Each staggered sea quark comes in four tastes, and each Ginsparg-Wilson valence quark owns a bosonic ghost partner, and these bosons are expressed by the field

$$\Sigma = \exp(2i\Phi/f),$$

which is an element of $U(4N_S + N_V|N_V)$, and Φ is a matrix gathering pseudoscalar fields. For instance, in the case $N_V = 3$, $N_S = 3$ ¹, the fields are arranged by [30, 32]

$$\Phi = \begin{pmatrix} U & \pi^+ & K^+ & Q_{ux} & Q_{uy} & Q_{uz} & \cdots & \cdots & \cdots \\ \pi^- & D & K^0 & Q_{dx} & Q_{dy} & Q_{dz} & \cdots & \cdots & \cdots \\ K^- & \bar{K}^0 & S & Q_{sx} & Q_{sy} & Q_{sz} & \cdots & \cdots & \cdots \\ Q_{ux}^\dagger & Q_{dx}^\dagger & Q_{sx}^\dagger & X & P^+ & T^+ & R_{xx}^\dagger & R_{yx}^\dagger & R_{zx}^\dagger \\ Q_{uy}^\dagger & Q_{dy}^\dagger & Q_{sy}^\dagger & P^- & Y & T^0 & R_{xy}^\dagger & R_{yy}^\dagger & R_{zy}^\dagger \\ Q_{uz}^\dagger & Q_{dz}^\dagger & Q_{sz}^\dagger & T^- & \bar{T}^0 & Z & R_{xz}^\dagger & R_{yz}^\dagger & R_{zz}^\dagger \\ \cdots & \cdots & \cdots & R_{xx} & R_{xy} & R_{xz} & \tilde{X} & \tilde{P}^+ & \tilde{T}^+ \\ \cdots & \cdots & \cdots & R_{yx} & R_{yy} & R_{yz} & \tilde{P}^- & \tilde{Y} & \tilde{T}^0 \\ \cdots & \cdots & \cdots & R_{zx} & R_{zy} & R_{zz} & \tilde{T}^- & \tilde{T}^0 & \tilde{Z} \end{pmatrix},$$

where we label sea quarks by u, d , and s and corresponding valence quarks and valence ghosts by x, y, z and $\tilde{x}, \tilde{y}, \tilde{z}$, respectively. The sea-quark bound state fields are $U, \pi^+, K^+, \text{etc.}, P^+, T^+, T^0, X, Y$ and Z are the $x\bar{y}, x\bar{z}, y\bar{z}, x\tilde{x}, y\tilde{y}$ and $z\tilde{z}$ valence bound states, respectively; $\tilde{P}^+, \tilde{T}^+, \tilde{T}^0, \tilde{X}, \tilde{Y}$ and \tilde{Z} are the relevant combinations of valence ghost quarks. Those labeled by R 's are the (fermionic) bound state composed of one valence and one ghost quark. Similarly, Q_{Fv} stands for the bosonic mixed bound state $F\bar{v}$, where $F \in \{u, d, s\}$, and $v \in \{x, y, z\}$. The mixed ghost-sea pseudo-Goldstone bosons indicated by ellipses are not used in this work.

The valence-valence mesons satisfy mass relations [30]:

$$M_{vv'}^2 = \mu(m_v + m_{v'}), \quad (1)$$

where three valence quarks have m_x, m_y and m_z (same for the corresponding valence ghost flavors), respectively. In this work we are only interested in the degenerate up and down valence quarks masses, to be specific, $m_x = m_y \neq m_z$ ($2+1$) case.

For a meson of taste b made up of sea quarks F and F' ($F \neq F'$), the tree-level results give [26]

$$M_{FF',b}^2 = \mu(m_F + m_{F'}) + a^2\Delta(\xi_b), \quad (2)$$

where the staggered sea quarks $4u, 4d, 4s$ own masses m_u, m_d and m_s , respectively, and Δ_t is different for each of the $SO(4)$ -taste irreps: P, V, A, T, I [26]. A new operator in the mixed action Lagrangian relates the valence and sea sectors and contributes a taste breaking parameter $a^2\Delta_{\text{Mix}}$ of the valence-sea pion mass [30]. For a $F\bar{v}$ meson with field Q_{Fv} , its mass is given by [30]

$$M_{Fv}^2 = \mu(m_F + m_v) + a^2\Delta_{\text{Mix}}, \quad (3)$$

where parameter Δ_{Mix} can be measured via lattice QCD.

The connected propagators for valence-valence mesons with $v, v' = x, y, z, \tilde{x}, \tilde{y}, \tilde{z}$ are given [30]

$$\langle \Phi_{vv'} | \Phi_{v'v} \rangle = \frac{\epsilon_x}{k^2 + M_{v,v'}^2}, \quad \epsilon_{x,y,z} = 1, \epsilon_{\tilde{x},\tilde{y},\tilde{z}} = -1. \quad (4)$$

MA χ PT has flavor-neutral quark-disconnected hairpin propagators involving double pole contributions. The flavor-neutral propagators appearing in the expression for the bubble contributions to scalar mesons are only those with two valence quarks [30],

$$\langle \Phi_{vv'} | \Phi_{v'v'} \rangle_{\text{disc}} = -\frac{1}{3} \frac{(k^2 + M_{U_I}^2)(k^2 + M_{S_I}^2)}{(k^2 + M_{v,v}^2)(k^2 + M_{v',v'}^2)(k^2 + M_{\eta_I}^2)}, \quad (5)$$

where it is convenient to use $m_0^2 \rightarrow \infty$ to decouple the η_I , and we are only interested in $2+1$ case [16],

$$m_{\pi_I^0}^2 = m_{U_I}^2 = m_{D_I}^2, \quad m_{\eta_I}^2 = \frac{1}{3}m_{U_I}^2 + \frac{2}{3}m_{S_I}^2,$$

here $M_{U_I}^2 = M_{U_5}^2 + a^2\Delta_I$, $M_{S_I}^2 = M_{S_5}^2 + a^2\Delta_I$. It is interesting to note that the sea-sea pseudo-Goldstone bosons in the above expressions are taste singlets.

The propagators for valence-sea mesons with $F = u, d, s$ and $v = x, y, z$ are given

$$\langle \Phi_{vF} | \Phi_{Fv} \rangle = \frac{1}{k^2 + M_{v,F}^2}. \quad (6)$$

It is important to note that propagators (4), (5) and (6) rest only on taste breaking parameters $a^2\Delta_I$ and $a^2\Delta_{\text{Mix}}$.

III. SCALAR BUBBLE TERM IN MA χ PT

The simulations with chiral valence quarks on top of the MILC staggered sea quarks is feasible and charming. The relevant effective theory has been developed [30]. Following the original derivations and notations in Refs. [17, 30–32], we here deduce the bubble contributions to the κ and σ correlators in M χ PT with $2+1$ chiral valence quarks and $2+1$ MILC staggered sea quarks ($m_u = m_d \neq m_s$). Since the relevant a_0 bubble contribution is derived in Ref. [17], and its time Fourier transform is provided in Eq. (11) of Ref. [31], in this work we will directly quote these results.

¹ These fields, which are first provided to study $\pi\pi$ scattering [32], explicitly include strange valence and strange ghost quark.

A. κ bubble

The bubble contribution to κ correlator is denoted in Ref. [23]. Applying the Wick contractions, we have [17]²

$$B_{2+1,\kappa}^{\text{M}\chi\text{PT}} = \mu^2 \left[2 \langle \Phi_{xx} | \Phi_{zz} \rangle \langle \Phi_{xz} | \Phi_{zx} \rangle + \sum_{v=x,y,z,\tilde{x},\tilde{y},\tilde{z}} \langle \Phi_{xv} | \Phi_{vx} \rangle \langle \Phi_{vz} | \Phi_{zv} \rangle + \sum_{F=u,d,s} \langle \Phi_{xF} | \Phi_{Fx} \rangle \langle \Phi_{Fz} | \Phi_{zF} \rangle \right], \quad (7)$$

where the third term is already considered to reduce four tastes per sea quark to one. The bubble contribution is secured by inserting relevant propagators into (7)

$$B_{2+1,\kappa}^{\text{M}\chi\text{PT}}(p) = \mu^2 \sum_k \left\{ -\frac{1}{(k+p)^2 + M_{x,z}^2} \times \left[\frac{2}{3} \frac{1}{(k^2 + M_{x,x}^2)(k^2 + M_{z,z}^2)} \frac{(k^2 + M_{U_I}^2)(k^2 + M_{S_I}^2)}{k^2 + M_{\eta_I}^2} + \frac{1}{3} \frac{1}{(k^2 + M_{x,x}^2)^2} \frac{(k^2 + M_{U_I}^2)(k^2 + M_{S_I}^2)}{k^2 + M_{\eta_I}^2} + \frac{1}{3} \frac{1}{(k^2 + M_{z,z}^2)^2} \frac{(k^2 + M_{U_I}^2)(k^2 + M_{S_I}^2)}{k^2 + M_{\eta_I}^2} \right] + 2 \frac{1}{(k+p)^2 + M_{x,u}^2} \frac{1}{k^2 + M_{z,u}^2} + \frac{1}{(k+p)^2 + M_{x,s}^2} \frac{1}{k^2 + M_{z,s}^2} \right\}. \quad (8)$$

It is helpful to perform a partial fraction decomposition, then Eq. (8) can be simplified to a form

$$B_{2+1,\kappa}^{\text{M}\chi\text{PT}}(p) = \mu^2 \sum_k \left\{ -\frac{1}{(k+p)^2 + M_{x,z}^2} \times \left[\frac{g_1}{k^2 + M_{\eta_I}^2} + \frac{g_2}{k^2 + M_{x,x}^2} + \frac{g_3}{k^2 + M_{z,z}^2} + \frac{g_4}{(k^2 + M_{x,x}^2)^2} + \frac{g_5}{(k^2 + M_{z,z}^2)^2} \right] + \frac{2}{(k+p)^2 + M_{x,u}^2} \frac{1}{k^2 + M_{z,u}^2} + \frac{1}{(k+p)^2 + M_{x,s}^2} \frac{1}{k^2 + M_{z,s}^2} \right\}, \quad (9)$$

² It is interesting and important to note that the corresponding bubble contribution to a_0 correlator is

$$B_{2+1,a_0}^{\text{M}\chi\text{PT}} = \mu^2 \left[\sum_{F=u,d,s} \langle \Phi_{xF} | \Phi_{Fx} \rangle \langle \Phi_{Fy} | \Phi_{yF} \rangle + 2 \langle \Phi_{xx} | \Phi_{yy} \rangle \langle \Phi_{xy} | \Phi_{yx} \rangle + \sum_{v=x,y,z,\tilde{x},\tilde{y},\tilde{z}} \langle \Phi_{xv} | \Phi_{vx} \rangle \langle \Phi_{vy} | \Phi_{yv} \rangle \right],$$

which results in two extra terms to original Eq. (13) in Ref. [17], which are neatly canceled each other out in the final a_0 bubble. Consequently, it is nicely consistent with Sasa's result derived with 2 chiral valence quarks and 2 + 1 staggered sea quarks [17].

where

$$\begin{aligned} g_1 &= \frac{1}{3} \times \frac{(M_{U_I}^2 - M_{\eta_I}^2)(M_{S_I}^2 - M_{\eta_I}^2)}{(M_{x,x}^2 - M_{\eta_I}^2)(M_{z,z}^2 - M_{\eta_I}^2)} \\ &\times \left[2 + \frac{M_{z,z}^2 - M_{\eta_I}^2}{M_{x,x}^2 - M_{\eta_I}^2} + \frac{M_{x,x}^2 - M_{\eta_I}^2}{M_{z,z}^2 - M_{\eta_I}^2} \right], \\ g_2 &= \frac{2}{3} \times \frac{(M_{U_I}^2 - M_{x,x}^2)(M_{S_I}^2 - M_{x,x}^2)}{(M_{\eta_I}^2 - M_{x,x}^2)(M_{z,z}^2 - M_{x,x}^2)} \\ &+ \frac{3M_{x,x}^2(M_{x,x}^2 - 2M_{\eta_I}^2) + 2M_{S_I}^4 + M_{U_I}^4}{9(M_{\eta_I}^2 - M_{x,x}^2)^2}, \\ g_3 &= \frac{2}{3} \times \frac{(M_{U_I}^2 - M_{z,z}^2)(M_{S_I}^2 - M_{z,z}^2)}{(M_{\eta_I}^2 - M_{z,z}^2)(M_{x,x}^2 - M_{z,z}^2)} \\ &+ \frac{3M_{z,z}^2(M_{z,z}^2 - 2M_{\eta_I}^2) + 2M_{S_I}^4 + M_{U_I}^4}{9(M_{\eta_I}^2 - M_{z,z}^2)^2}, \\ g_4 &= \frac{(M_{U_I}^2 - M_{x,x}^2)(M_{S_I}^2 - M_{x,x}^2)}{3(M_{\eta_I}^2 - M_{x,x}^2)}, \\ g_5 &= \frac{(M_{U_I}^2 - M_{z,z}^2)(M_{S_I}^2 - M_{z,z}^2)}{3(M_{\eta_I}^2 - M_{z,z}^2)}. \end{aligned} \quad (10)$$

The time Fourier transform of this bubble contribution (namely, $B_{2+1,\kappa}^{\text{M}\chi\text{PT}}(t) = F.T.[B_{2+1,\kappa}^{\text{M}\chi\text{PT}}(p)]_{\mathbf{p}=0}$) is then provided by

$$B_{2+1,\kappa}^{\text{M}\chi\text{PT}}(t) = \frac{\mu^2}{4L^3} \sum_{\mathbf{k}} \left[-g_1 \frac{e^{-(\omega_{xz} + \omega_{\eta_I})t}}{\omega_{xz}\omega_{\eta_I}} - g_2 \frac{e^{-(\omega_{xz} + \omega_{xx})t}}{\omega_{xx}\omega_{xz}} - g_3 \frac{e^{-(\omega_{xz} + \omega_{zz})t}}{\omega_{xz}\omega_{zz}} - g_4 \frac{e^{-(\omega_{xz} + \omega_{xx})t}}{2\omega_{xz}\omega_{xx}^3} (\omega_{xx}t + 1) - g_5 \frac{e^{-(\omega_{xz} + \omega_{zz})t}}{2\omega_{xz}\omega_{zz}^3} (\omega_{zz}t + 1) + \frac{e^{-(\omega_{xs} + \omega_{zs})t}}{\omega_{xs}\omega_{zs}} + 2 \frac{e^{-(\omega_{xu} + \omega_{zu})t}}{\omega_{xu}\omega_{zu}} \right], \quad (11)$$

where, for brevity, in this work we use the notation $\omega_i \equiv \sqrt{\mathbf{k}^2 + m_i^2}$ from Ref. [31].

It is worth mentioning that no free parameters are presented in (11), which is solely predicted by M χ PT. The meson masses and coupling constant μ are evaluated from lattice studies [16]. The values of mixed-meson splittings $a^2\Delta_{\text{mix}}$ and taste-singlet breaking $a^2\Delta_I$ will be quoted from Refs. [16, 31]. Additionally, we notice that equation (11) gets unphysical contributions from KS intermediate states not presenting in continuum full QCD. Luckily, it never dominates κ bubble contribution at large t even if the valence quark masses are enough small, which make κ mass relatively safe to be determined, while it is difficult to extract a_0 mass since unphysical $\pi\pi$ intermediate states dominate a_0 correlator. Moreover, there are two double poles in its momentum-space propagator, which lead to the infrared-sensitive linear-in- t growth factors in the fourth and fifth terms of Eq. (11). We will observe that there is a desirable cancellation between two double poles for a generic mass tuning.

The KS intermediate states contribute to κ bubble (11) if lattice theory (e.g., M χ PT) is not unitary. Since

full QCD is restored in MA χ PT only in the continuum limit, the unphysical KS contributions can not be entirely removed for any selection of mixed-action realistic simulation parameters. In the continuum limit ($a^2\Delta_I \rightarrow 0$, $a^2\Delta_{\text{Mix}} \rightarrow 0$), the expression (11) reduces to a pretty simple form

$$B_\kappa^{a=0}(t) = \frac{\mu^2}{4L^3} \sum_{\mathbf{k}} \left[\frac{3}{2} \frac{e^{-(\omega_{U_5} + \omega_{K_5})t}}{\omega_{U_5}\omega_{K_5}} + \frac{1}{6} \frac{e^{-(\omega_{K_5} + \omega_{\eta_5})t}}{\omega_{K_5}\omega_{\eta_5}} \right], \quad (12)$$

which is nicely consistent with the corresponding S χ PT result, which is written down in (A1). The desired physical contributions $e^{-(M_\pi + M_K)t}$ certainly dominate at large t with $a \neq 0$.

B. σ bubble

The bubble contribution to σ correlator is denoted in Ref. [19]. Applying the Wick contractions, we get [17]

$$\begin{aligned} B_{2+1,\sigma}^{\text{M}\chi\text{PT}} = & \mu^2 \left[2 \langle \Phi_{xx} | \Phi_{xx} \rangle \langle \Phi_{xx} | \Phi_{xx} \rangle \right. \\ & + 2 \langle \Phi_{xx} | \Phi_{yy} \rangle \langle \Phi_{xx} | \Phi_{yy} \rangle \\ & + \sum_{v=x,y,z,\bar{x},\bar{y},\bar{z}} \langle \Phi_{xv} | \Phi_{vx} \rangle \langle \Phi_{vv} | \Phi_{vv} \rangle \\ & \left. + \sum_{F=u,d,s} \langle \Phi_{1F} | \Phi_{F1} \rangle \langle \Phi_{2F} | \Phi_{F2} \rangle \right]. \quad (13) \end{aligned}$$

The bubble contribution is secured by plugging the relevant propagators into (13)

$$\begin{aligned} B_{2+1,\sigma}^{\text{M}\chi\text{PT}}(p) = & \mu^2 \sum_{\mathbf{k}} \left\{ -\frac{4}{3} \frac{1}{(k+p)^2 + M_{x,x}^2} \right. \\ & \times \frac{1}{(k^2 + M_{x,x}^2)^2} \frac{(k^2 + M_{U_I}^2)(k^2 + M_{S_I}^2)}{k^2 + M_{\eta_I}^2} \\ & + \frac{4}{9} \frac{1}{((k+p)^2 + M_{x,x}^2)^2} \frac{((k+p)^2 + M_{U_I}^2)((k+p)^2 + M_{S_I}^2)}{(k+p)^2 + M_{\eta_I}^2} \\ & \times \frac{1}{(k^2 + M_{x,x}^2)^2} \frac{(k^2 + M_{U_I}^2)(k^2 + M_{S_I}^2)}{k^2 + M_{\eta_I}^2} \\ & + 2 \frac{1}{(k+p)^2 + M_{x,x}^2} \frac{1}{(k^2 + M_{x,x}^2)^2} \\ & + 2 \frac{1}{(k+p)^2 + M_{x,u}^2} \frac{1}{k^2 + M_{x,u}^2} \\ & \left. + \frac{1}{(k+p)^2 + M_{x,s}^2} \frac{1}{k^2 + M_{x,s}^2} \right\}. \quad (14) \end{aligned}$$

It is worth mentioning that σ bubble in MA χ PT is much simpler than that of the corresponding S χ PT result [19], as expected. It is convenient to use the partial fraction decomposition, then expression (14) can be simplified to a compact form

$$B_{2+1,\sigma}^{\text{M}\chi\text{PT}}(p) = B^2 \sum_{\mathbf{k}} \left\{ \frac{h_1}{(k+p)^2 + M_{x,x}^2} \frac{1}{k^2 + M_{x,x}^2} \right.$$

$$\begin{aligned} & + \frac{h_2}{(k+p)^2 + M_{x,x}^2} \frac{1}{(k^2 + M_{x,x}^2)^2} \\ & + \frac{h_3}{(k+p)^2 + M_{x,x}^2} \frac{1}{k^2 + M_{\eta_I}^2} \\ & + \frac{h_4}{((k+p)^2 + M_{x,x}^2)^2} \frac{1}{(k^2 + M_{x,x}^2)^2} \\ & + \frac{h_5}{(k+p)^2 + M_{\eta_I}^2} \frac{1}{k^2 + M_{\eta_I}^2} \\ & + \frac{h_6}{((k+p)^2 + M_{x,x}^2)^2} \frac{1}{k^2 + M_{\eta_I}^2} \\ & + 2 \frac{1}{(k+p)^2 + M_{x,u}^2} \frac{1}{k^2 + M_{x,u}^2} \\ & \left. + \frac{1}{(k+p)^2 + M_{x,s}^2} \frac{1}{k^2 + M_{x,s}^2} \right\}, \quad (15) \end{aligned}$$

where

$$\begin{aligned} h_1 = & 2 - \frac{4}{3} \frac{3M_{x,x}^2(M_{x,x}^2 - 2M_{\eta_I}^2) + 2M_{S_I}^4 + M_{U_I}^4}{3(M_{\eta_I}^2 - M_{x,x}^2)^2} \\ & + \frac{4}{9} \left(\frac{3M_{x,x}^2(M_{x,x}^2 - 2M_{\eta_I}^2) + 2M_{S_I}^4 + M_{U_I}^4}{3(M_{\eta_I}^2 - M_{x,x}^2)^2} \right)^2, \\ h_2 = & \frac{(M_{U_I}^2 - M_{x,x}^2)(M_{S_I}^2 - M_{x,x}^2)}{M_{\eta_I}^2 - M_{x,x}^2} \times \\ & \left(\frac{8}{9} \frac{3M_{x,x}^2(M_{x,x}^2 - 2M_{\eta_I}^2) + 2M_{S_I}^4 + M_{U_I}^4}{3(M_{\eta_I}^2 - M_{x,x}^2)^2} - \frac{4}{3} \right), \\ h_3 = & \frac{(M_{U_I}^2 - M_{\eta_I}^2)(M_{S_I}^2 - M_{\eta_I}^2)}{(M_{x,x}^2 - M_{\eta_I}^2)^2} \times \\ & \left(\frac{8}{9} \frac{3M_{x,x}^2(M_{x,x}^2 - 2M_{\eta_I}^2) + 2M_{S_I}^4 + M_{U_I}^4}{3(M_{\eta_I}^2 - M_{x,x}^2)^2} - \frac{4}{3} \right), \\ h_4 = & \frac{4}{9} \left(\frac{(M_{U_I}^2 - M_{x,x}^2)(M_{S_I}^2 - M_{x,x}^2)}{M_{\eta_I}^2 - M_{x,x}^2} \right)^2, \\ h_5 = & \frac{4}{9} \left(\frac{(M_{U_I}^2 - M_{\eta_I}^2)(M_{S_I}^2 - M_{\eta_I}^2)}{(M_{x,x}^2 - M_{\eta_I}^2)^2} \right)^2, \\ h_6 = & \frac{8}{9} \frac{(M_{U_I}^2 - M_{x,x}^2)(M_{S_I}^2 - M_{x,x}^2)}{M_{\eta_I}^2 - M_{x,x}^2} \\ & \times \frac{(M_{U_I}^2 - M_{\eta_I}^2)(M_{S_I}^2 - M_{\eta_I}^2)}{(M_{x,x}^2 - M_{\eta_I}^2)^2}. \quad (16) \end{aligned}$$

The time Fourier transform of this bubble correlator (namely $B_{2+1,\sigma}^{\text{M}\chi\text{PT}}(t) = \text{F.T.}[B_{2+1,\sigma}^{\text{M}\chi\text{PT}}(p)]_{\mathbf{p}=0}$) is then provided by

$$\begin{aligned} B_{2+1,\sigma}^{\text{M}\chi\text{PT}}(t) = & \frac{\mu^2}{4L^3} \sum_{\mathbf{k}} \left[h_1 \frac{e^{-2\omega_{xx}t}}{\omega_{xx}^2} + h_2 \frac{e^{-2\omega_{xx}t}}{2\omega_{xx}^4} (\omega_{xx}t + 1) \right. \\ & + h_3 \frac{e^{-(\omega_{xx} + \omega_{\eta_I})t}}{\omega_{xx}\omega_{\eta_I}} + h_4 \frac{e^{-2\omega_{xx}t}}{4\omega_{xx}^6} (\omega_{xx}t + 1)^2 \\ & + h_5 \frac{e^{-2\omega_{\eta_I}t}}{\omega_{\eta_I}^2} + h_6 \frac{e^{-(\omega_{xx} + \omega_{\eta_I})t}}{2\omega_{xx}^3\omega_{\eta_I}} (\omega_{xx}t + 1) \\ & \left. + 2 \frac{e^{-2\omega_{xu}t}}{\omega_{xu}^2} + \frac{e^{-2\omega_{xs}t}}{\omega_{xs}^2} \right]. \quad (17) \end{aligned}$$

Once again, we note that no free parameters are presented in (17), which is solely predicted by MA χ PT. The expression (17) also gets unphysical contributions from $\pi\eta$ intermediate states, which luckily never dominate σ correlator at large t even if the valence quark masses are enough small. Moreover, there are two kind of double poles in its momentum-space propagator: the infrared-sensitive linear-in- t growth factors in the fourth and sixth terms of Eq. (17) arising from the double poles, and the strong infrared-sensitive quadratic-in- t^2 growth factor in the fourth term of Eq. (17) stemming from the multiplication of two double poles. We will observe the fourth term of Eq. (17) plays a key role in σ bubble.

The unphysical $\pi\eta$ intermediate states contribute to σ bubble (17) since MA χ PT is not unitary at $a = 0$. The unphysical $\pi\eta$ contributions can not be neatly removed for any selection of mixed-action realistic simulation parameters. In the continuum limit ($a^2\Delta_I \rightarrow 0$, $a^2\Delta_{\text{Mix}} \rightarrow 0$), the expression (17) reduces to a pretty simple form

$$B_{2+1,\sigma}^{\text{M}\chi\text{PT}}(t) = \frac{\mu^2}{4L^3} \sum_{\mathbf{k}} \left[3 \frac{e^{-2\omega_{U_5}t}}{\omega_{U_5}^2} + \frac{e^{-2\omega_{K_5}t}}{\omega_{K_5}^2} + \frac{1}{9} \frac{e^{-2\omega_{\eta a_5}t}}{\omega_{\eta_5}^2} \right], \quad (18)$$

which is elegantly consistent with the corresponding S χ PT result, which is courteously written down in (A2). Without doubt, away from the continuum limit, the wanted physical contributions $e^{-2M_\pi t}$ will dominate σ bubble at large t .

IV. NUMERICAL ILLUSTRATION OF BUBBLE CONTRIBUTIONS

We plan on launching a serial of the mixed action lattice investigations of scalar mesons using DW fermions on top of the MILC 2+1 asqtad-improved staggered sea quarks. So far, the MILC lattice ensembles with two lattice spacings: the MILC coarse lattices and MILC fine lattices are extensively studied. Therefore, it is very useful to exploit the known parameters determined by MILC collaboration on these lattices [16] to acquire the preliminary numerical predictions for the bubble contributions to scalar mesons in MA χ PT, which then will guide us in the ongoing lattice investigations with the reasonable and economical mass tuning between the valence quarks and sea quarks.

We illustrate these predictions only on two MILC lattice ensembles: one is a coarse ensemble ($a \approx 0.12$ fm, $am_u/am_s = 0.005/0.05$), another one is a fine ensemble ($a \approx 0.09$ fm, $am_u/am_s = 0.0062/0.031$), which are in this work labeled “coarse” and “fine” lattice ensemble, respectively. The taste-singlet breaking $a^2\Delta_I$ of sea-sea π mass is acquired from MILC determinations [16], and taste breaking parameter $a^2\Delta_{\text{Mix}}$ of valence-sea π mass is quoted from Aubin *et al*’s measurements [31].

Considering that MA χ PT violates unitarity at $a \neq 0$, in principle, we can make a huge of choices, and can not prefer one mass matching to another for a priori reason. Nonetheless, all tuning choices are identical at $a = 0$. Therefore, we just exhibit two most popular mass matchings of chiral valence quarks and staggered sea quarks. To help one quantitatively comprehend each term in the bubble contributions to scalar mesons, each of them is displayed in the corresponding figures, and indicate the whole bubble contribution with black solid line.

A. Matching 1

The first selection is to fix the valence pion mass and kaon mass to be equal to the taste-pseudoscalar sea pion mass and kaon mass, to be specific, $M_{x,x} = M_{U_5}$, which is practiced in Ref. [37], and $M_{x,z} = M_{K_5}$. This tuning is attractive since the taste-pseudoscalar pion mass disappears in the chiral limit, even at $a \neq 0$. Nonetheless, this choice increases unitarity-violation for the bubble contributions to scalar mesons due to large taste-singlet breaking $a^2\Delta_I$ on the coarse MILC lattices.

Figures 1 and 2 show κ bubble on the MILC coarse and fine ensembles, respectively. In these figures, “ πK ” indicates the intermediate states with the valence pion and kaon, and likewise for “ $K\eta$ ” and “ KS ”, while “ πK Mixed” represents the intermediate states with the mixed valence-sea pion and kaon, and likewise for “ KS Mixed”. “ πK double pole” and “ KS double pole” are the fourth and fifth terms in (17). The analogous notations are employed to σ and a_0 bubbles in the corresponding figures in this work.

From Figs. 1 and 2, we note that physical ηK states dominate κ bubble until $t \approx 11$ for coarse lattice and $t \approx 27$ for fine lattice and quickly decrease after that. On the other hand, “ πK double pole” is pretty small at small t , but for enough large t it gradually dominates κ bubble, whereas “ KS double pole” is negligible, and it is important to note that there is a cancelation between two double pole terms, which is a special feature of the κ bubble, and this cancelation is a good news for studying κ meson since it decreases the unitarity-violation of κ bubble. Moreover, the πK state plays an important in κ bubble, and it is important to note that unphysical KS state never dominate κ bubble.

Figures 3 and 4 show a_0 bubble on the MILC coarse and fine ensembles, respectively. We note that physical $\pi\eta$ states dominate a_0 bubble until $t \approx 4$ for coarse lattice and $t \approx 12$ for fine lattice, and quickly decrease after that. On the other hand, the third term in Eq. (11) of Ref. [31] (“ $\pi\pi$ double pole”) is pretty small at small t , but for enough large t it eventually dominates a_0 bubble. It is important to note that physical KK state never dominate a_0 bubble, while unphysical $\pi\pi$ state plays a very important role in a_0 bubble. This indicates that the reliable determination of a_0 meson mass is feasible only for appropriate quark masses and times [17].

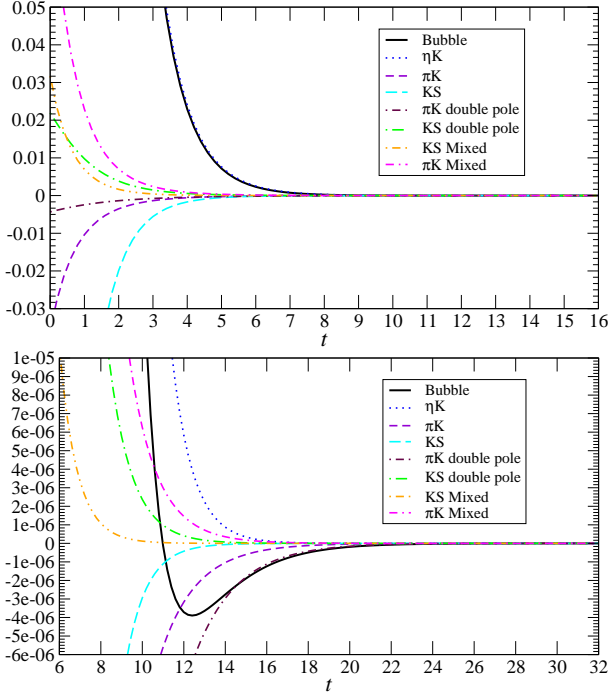


FIG. 1: κ bubble (11) for the simulation with chiral fermions on a MILC “coarse” staggered configuration. The valence and sea quark masses are tuned by matching $M_{x,x} = M_{U_5}$ and $M_{x,z} = M_{K_5}$. The parameters $a^2\Delta_I$ and $a^2\Delta_{\text{Mix}}$ are taken from Refs. [16], [31], respectively. The top panel shows the data on the small t range, while bottom panel indicates the data on the large t range.

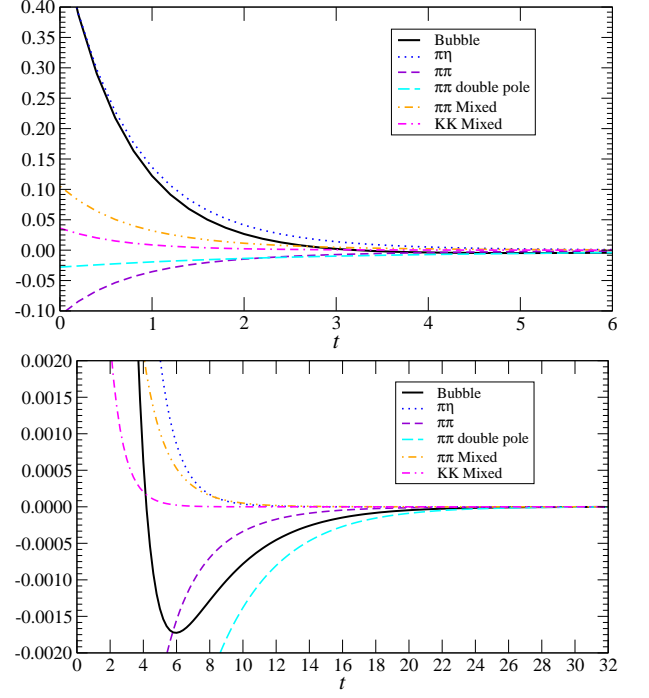


FIG. 3: a_0 bubble (Eq. (11) of Ref. [31]) for a simulation with chiral fermions on a MILC coarse staggered configuration. The valence and sea quark masses are tuned as $M_{x,x} = M_{U_5}$. The top panel shows the data on the small t range, while bottom panel indicates the data on the large t range. “ $\pi\pi$ double pole” is the third term in Eq. (11) of Ref. [31].

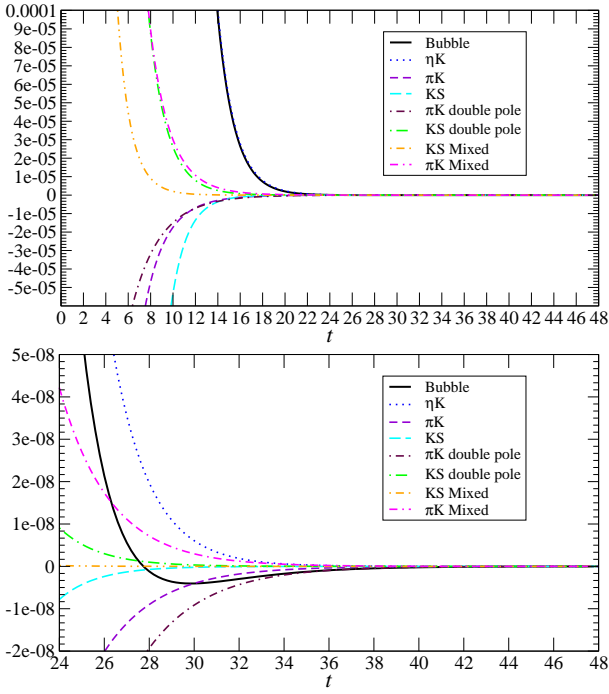


FIG. 2: Same as Fig. 1, but with chiral fermions on a MILC staggered fine lattice ensemble.

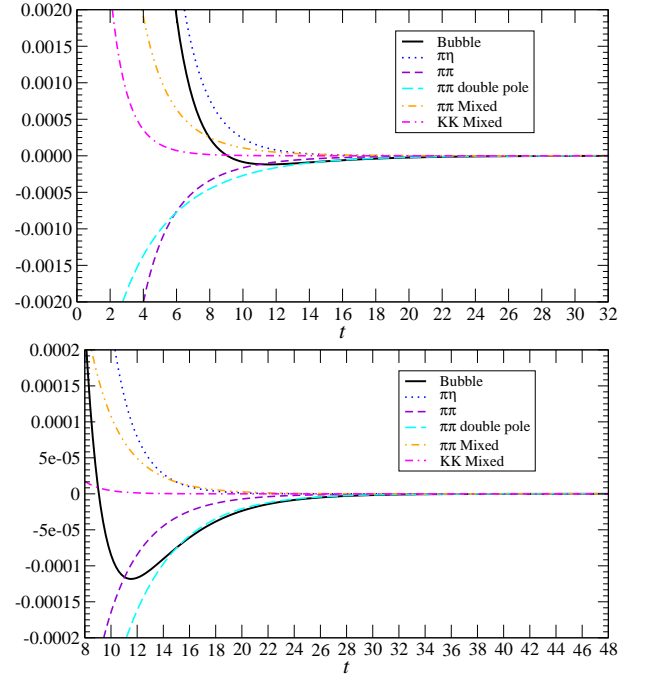


FIG. 4: Same as Fig. 3, but with chiral fermions on a MILC staggered fine lattice ensemble.

Figures 5 and 6 show σ bubble on the MILC coarse and fine ensembles, respectively. We note that physical $\pi\pi$ states (the second term in (17)) dominates σ bubble until $t \approx 3$ for coarse lattice and $t \approx 8$ for fine lattice. On the other hand, the fourth term in (17) (“ $\pi\pi$ two double pole”) is pretty small at small t ³, but for enough large t it eventually dominates σ bubble⁴. While the sixth term in (17) (“ $\pi\eta$ double pole”) is negligible, and it is obvious to note that there exists a cancelation among three term with double poles. Moreover, it is important to note that the unphysical $\pi\eta$ state never dominate σ bubble, and σ bubble is positive for all time.

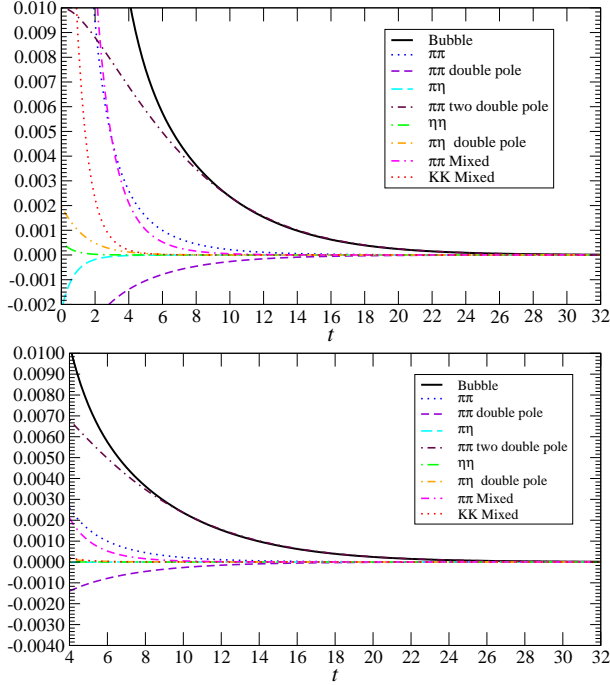


FIG. 5: σ bubble (17) for a simulation with chiral fermions on a MILC coarse staggered configuration. The valence and sea quark masses are tuned as $M_{x,x} = M_{U_5}$.

It is worth mentioning that all the bubble contributions to scalar correlators are dominated by the double poles at large t for this tuning. Actually the double pole is an unphysical effect which stems from selecting the valence-quark action different from the sea-quark action [36]. We found that these unitarity violations are not likely to be fairly small for this tuning on MILC coarse lattice, while the degree of unitarity violation decreases with the finer lattice spacing, as we expected.

³ The coefficient of the factor quadratic-in- t^2 , which is denoted as h_4 in (16), is quite small for a typical lattice simulation [36]. It is about 0.005 for coarse lattice and 0.0007 for fine lattice.

⁴ It overwhelmingly dominates σ bubble as early as $t \approx 6$ for coarse lattice, and dominates σ bubble about $t \approx 16$ for fine lattice. It means that if we do not choose a suitable simulation parameters, this term will be “infrared-diaster” to σ bubble.

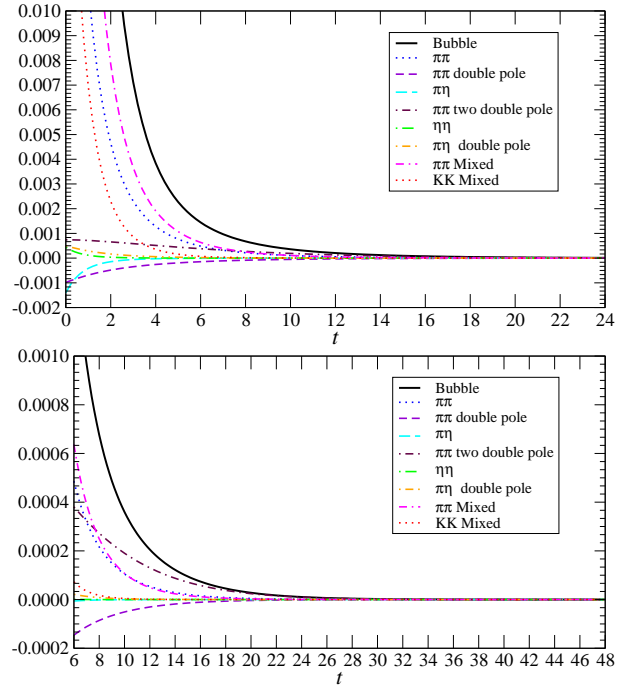


FIG. 6: Same as Fig. 5, but with chiral fermions on a MILC staggered fine lattice ensemble.

B. Matching 2

The second choice is to fix the valence pion mass and valence kaon mass to be equal to the taste-singlet sea pion mass U_I and taste-singlet sea kaon mass, respectively. To be specific, $M_{x,x} = M_{U_I}$ and $M_{x,z} = M_{K_I}$. This tuning one hundred per cent removes the double pole terms in both κ bubble in (11), σ bubble in (17), and a_0 bubble in Eq. (11) of Ref. [31]. Moreover, these bubble contributions are turned out to be relatively small and usually positive. Nonetheless it still does not entirely remove unphysical KS state in κ bubble in (11), $\pi\eta$ state in σ bubble in (17), and $\pi\pi$ state in a_0 bubble in Eq. (11) of Ref. [31]. Additionally, in practice this tuning may not be recommendable since it would lead to a fairly heavy valence pion and kaon on the MILC coarse lattices, as for the MILC fine, superfine, or ultrafine lattices, it is a different story.

Figure 7 and Figure 8 show κ bubble on a MILC coarse and fine ensemble, respectively. We note that physical πK states (the seventh term in (11)) dominate κ bubble at all time. Moreover, the unphysical KS state is small, and never dominate κ bubble, while physical $K\eta$ state make a small contribution to κ bubble.

Figure 9 displays σ bubble on a MILC coarse ensemble. We note that physical $\pi\pi$ states (the first term in (17)) dominate σ bubble at all time. Moreover, physical $\eta\eta$ and KK states play a small role in σ bubble.

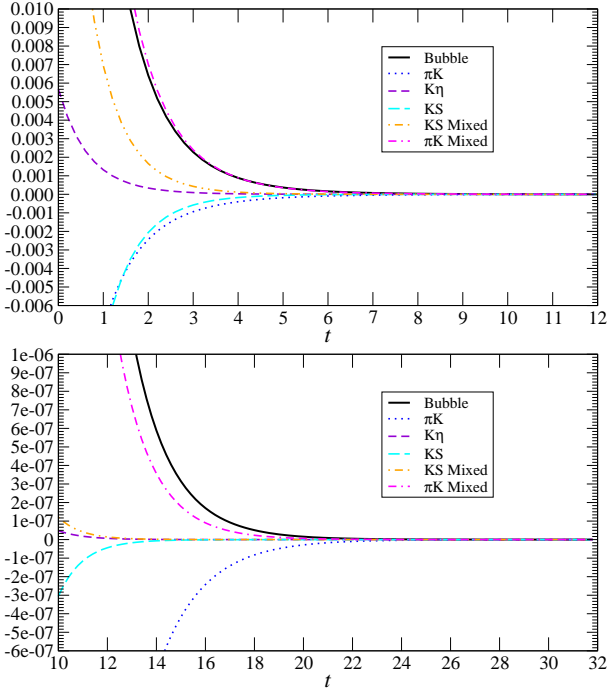


FIG. 7: κ bubble (11) for the simulation with chiral fermions on 2 + 1 MILC coarse staggered configuration. The valence and sea quark masses are tuned by matching $M_{x,x} = M_{U_I}$ and $M_{x,z} = M_{K_I}$.

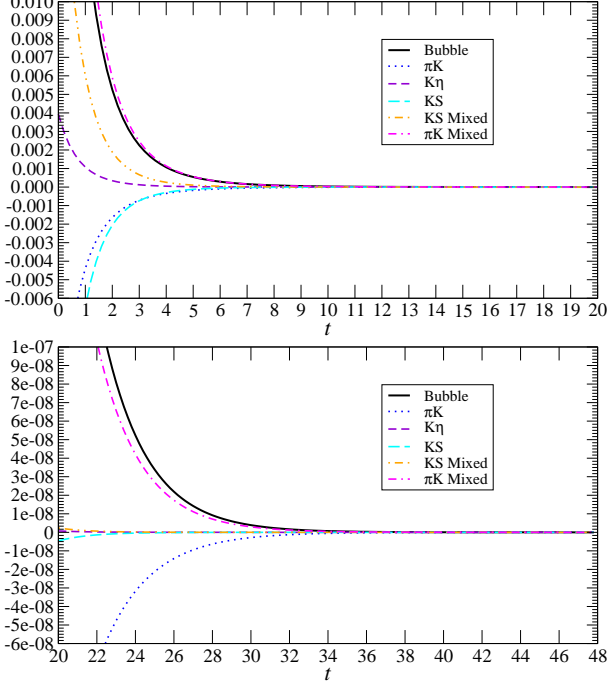


FIG. 8: Same as Fig. 7, but with chiral fermions on a MILC staggered fine lattice ensemble.

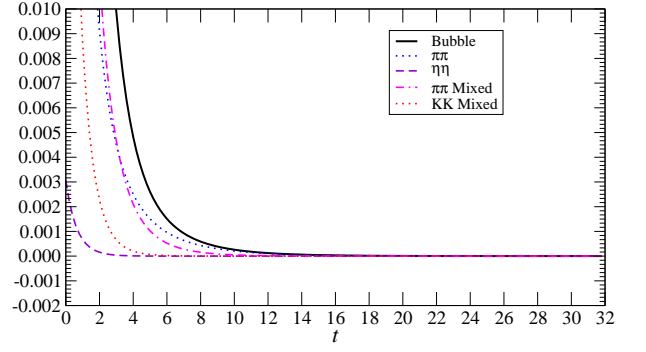


FIG. 9: σ bubble (17) for the simulation with chiral fermions on 2 + 1 MILC fine staggered configuration. The valence and sea quark masses are tuned as $M_{x,x} = M_{U_I}$.

V. SUMMARY

In this work we extended Sasa’s derivation on bubble contribution to a_0 correlator in $\text{MA}\chi\text{PT}$ [17] to those of κ and σ correlators. We found that these extensions are useful since κ and σ bubbles demonstrate many new features as compared with a_0 bubble. For example, the κ and σ bubbles are dominated by the physical two-particle states at enough large t , while a_0 bubble is dominated by unphysical two pions states. Moreover, we notice a strong infrared-sensitive quadratic-in- t^2 growth factor in the σ bubble due to the multiplication of two double poles, in practice, special attention should be paid to monitor the size of this unitarity violations, otherwise it leads to an “infrared-diaster” to σ bubble for a given tuning.

$\text{MA}\chi\text{PT}$ predicts the observed unitarity-violations pretty well, it is good news for one who employs the mixed actions to study scalar meson. Moreover, different mass tunings have remarkable effects on scalar correlators, our extended analytical expressions are helpful to aid researchers in selecting the appropriate simulation parameters for determining scalar meson masses.

Lattice studies of scalar mesons using DW valence quarks and staggered sea quarks contains the excellent traits of both fermion discretizations. The corresponding numerical results will be used as a cross-check with our lattice studies on scalar mesons with other methods [38]. Therefore, it will be interesting to measure the relevant lattice data to verify the $\text{MA}\chi\text{PT}$ formulae for κ and σ bubbles. We will appeal for computational resources to pursue this challenging enterprise.

Acknowledgments

We appreciate K. F. Liu for helping us with some knowledge about scalar meson, and bring us attention to domain-wall fermion. We benefit from the happy day of studying scalar mesons with Carleton DeTar, Claude Bernard and Sasa Prelovsek during my Ph.D.

Appendix A: Bubble contribution

The κ bubble term is [23, 24]

$$B_{2+1,\kappa}^{\text{S}\chi\text{PT}}(t) = \mu^2/(4L^3) \times \{f_B^\kappa(t) + f_V^\kappa(t) + f_A^\kappa(t)\},$$

$$f_V^\kappa(t) \equiv \sum_{\mathbf{k}} \frac{1}{2} \left\{ g_{V_\eta} \frac{e^{-(\omega_{K_V} + \omega_{\eta_V})t}}{\omega_{K_V} \omega_{\eta_V}} + g_{V_{\eta'}} \frac{e^{-(\omega_{K_V} + \omega_{\eta'_V})t}}{\omega_{K_V} \omega_{\eta'_V}} \right. \\ \left. - \frac{e^{-(\omega_{K_V} + \omega_{U_V})t}}{\omega_{K_V} \omega_{U_V}} - \frac{e^{-(\omega_{K_V} + \omega_{S_V})t}}{\omega_{K_V} \omega_{S_V}} \right\},$$

$$f_B^\kappa(t) \equiv \sum_{\mathbf{k}} \left\{ \frac{e^{-(\omega_{K_I} + \omega_{\eta_I})t}}{6\omega_{K_I} \omega_{\eta_I}} - \frac{e^{-(\omega_{K_I} + \omega_{U_I})t}}{2\omega_{K_I} \omega_{U_I}} - \frac{e^{-(\omega_{K_I} + \omega_{S_I})t}}{\omega_{K_I} \omega_{S_I}} \right. \\ \left. + \frac{1}{16} \sum_{b=1}^{16} \left(2 \frac{e^{-(\omega_{K_b} + \omega_{U_b})t}}{\omega_{K_b} \omega_{U_b}} + \frac{e^{-(\omega_{K_b} + \omega_{S_b})t}}{\omega_{K_b} \omega_{S_b}} \right) \right\},$$

where g_{V_η} , $g_{V_{\eta'}}$ are denoted in [23, 24], for $f_A^\kappa(t)$ we just require $V \rightarrow A$ in $f_V^\kappa(t)$. The σ bubble term is [6, 19, 22]

$$B_{2+1,\sigma}^{\text{S}\chi\text{PT}}(t) = \mu^2/(4L^3) \times \{f_B^\sigma(t) + f_V^\sigma(t) + f_A^\sigma(t)\}$$

$$f_V^\sigma(t) \equiv \sum_{\mathbf{k}} \left\{ -4 \frac{e^{-2\omega_{U_V}t}}{\omega_{U_V}^2} + C_{V_\eta}^2 \frac{e^{-2\omega_{\eta_V}t}}{\omega_{\eta_V}^2} \right.$$

$$+ C_{V_{\eta'}}^2 \frac{e^{-2\omega_{\eta'_V}t}}{\omega_{\eta'_V}^2} - 2C_{V_\eta} C_{V_{\eta'}} \frac{e^{-(\omega_{\eta_V} + \omega_{\eta'_V})t}}{\omega_{\eta_V} \omega_{\eta'_V}} \Big\},$$

$$f_B^\sigma(t) \equiv \sum_{\mathbf{k}} \left\{ \frac{1}{9} \frac{e^{-2\omega_{\eta_I}t}}{\omega_{\eta_I}^2} - \frac{e^{-2\omega_{U_I}t}}{\omega_{U_I}^2} \right. \\ \left. + \frac{1}{16} \sum_{b=1}^{16} \left(4 \frac{e^{-2\omega_{U_b}t}}{\omega_{U_b}^2} + \frac{e^{-2\omega_{K_b}t}}{\omega_{K_b}^2} \right) \right\},$$

where C_{V_η} , $C_{V_{\eta'}}$ are given in [6, 19, 22], for $f_A^\sigma(t)$ we just require $V \rightarrow A$ in $f_V^\sigma(t)$. In the continuum limit, the surviving thresholds at large t are

$$B_{2+1,\kappa}^{\text{S}\chi\text{PT}}(t) = \frac{\mu^2}{4L^3} \left\{ \frac{3}{2} \frac{e^{-(m_\pi + m_K)t}}{m_\pi m_K} + \frac{1}{6} \frac{e^{-(m_K + m_\eta)t}}{m_K m_\eta} \right\}. \quad (\text{A1})$$

$$B_{2+1,\sigma}^{\text{S}\chi\text{PT}}(t) = \frac{\mu^2}{4L^3} \left\{ 3 \frac{e^{-2m_\pi t}}{m_\pi^2} + \frac{e^{-2m_K t}}{m_K^2} + \frac{1}{9} \frac{e^{-2m_\eta t}}{m_\eta^2} \right\}. \quad (\text{A2})$$

-
- [1] J. Beringer *et al.* [Particle Data Group Collaboration], Phys. Rev. D **86**, 010001 (2012).
 - [2] N. Mathur *et al.*, Phys. Rev. D **76**, 114505 (2007).
 - [3] S. Prelovsek, C. Dawson, T. Izubuchi, K. Orginos and A. Soni, Phys. Rev. D **70**, 094503 (2004).
 - [4] C. McNeile *et al.*, Phys. Rev. D **74**, 014508 (2006)
 - [5] K. -F. Liu, Prog. Theor. Phys. Suppl. **168**, 160 (2007).
 - [6] Z. -W. Fu and C. DeTar, Chin. Phys. C **35**, 1079 (2011).
 - [7] S. Prelovsek, T. Draper, C. B. Lang, M. Limmer, K. -F. Liu, N. Mathur and D. Mohler, Phys. Rev. D **82**, 094507 (2010).
 - [8] M. G. Alford and R. L. Jaffe, Nucl. Phys. B **578**, 367 (2000).
 - [9] M. Loan, Z. -H. Luo and Y. -Y. Lam, Eur. Phys. J. C **57**, 579 (2008).
 - [10] C. Alexandrou, J. O. Daldrop, M. D. Brida *et al.*, arXiv:1212.1418 [hep-lat].
 - [11] M. Wagner, C. Alexandrou, J. O. Daldrop *et al.*, arXiv:1302.3389 [hep-lat].
 - [12] S. Prelovsek and D. Mohler, Phys. Rev. D **79**, 014503 (2009).
 - [13] K. Gottfried and V. F. Weisskopf, *Concepts Of Particle Physics. Vol. 2*, New York, USA: Oxford Univ. Pr. (1986) 191-608.
 - [14] V. N. Gribov, Eur. Phys. J. C **10** (1999) 91.
 - [15] E. B. Gregory, A. C. Irving, C. C. McNeile, S. Miller and Z. Sroczynski, PoS LAT **2005**, 027 (2006).
 - [16] C. W. Bernard *et al.*, Phys. Rev. D **64**, 054506 (2001); C. Aubin *et al.*, Phys. Rev. D **70**, 094505 (2004).
 - [17] S. Prelovsek, PoS LAT **2005**, 085 (2006); S. Prelovsek, Phys. Rev. D **73**, 014506 (2006).
 - [18] A. Bazavov *et al.*, Rev. Mod. Phys. **82**, 1349 (2010); C. Bernard *et al.* Phys. Rev. D **83**, 034503 (2011).
 - [19] C. Bernard, C. DeTar, Z. Fu and S. Prelovsek, Phys. Rev. D **76** (2007) 094504.
 - [20] Z. -W. Fu, Chin. Phys. Lett. **28**, 081202 (2011).
 - [21] Z. -W. Fu and C. DeTar, Chin. Phys. C **35**, 896 (2011).
 - [22] Z. Fu, 2006, UMI-32-34073 [arXiv:1103.1541 [hep-lat]].
 - [23] Z. -W. Fu, Chin. Phys. C **36**, 489 (2012).
 - [24] Z. Fu, Int. J. Mod. Phys. A **28**, 1350059 (2013).
 - [25] L. Susskind, Phys. Rev. D **16**, 3031 (1977).
 - [26] W. -J. Lee and S. R. Sharpe, Phys. Rev. D **60**, 114503 (1999); C. Aubin and C. Bernard, Phys. Rev. D **68**, 034014 (2003); C. Aubin and C. Bernard, Phys. Rev. D **68**, 074011 (2003); S. R. Sharpe and R. S. Van de Water, Phys. Rev. D **71**, 114505 (2005).
 - [27] D. B. Kaplan, Phys. Lett. B **288**, 342 (1992).
 - [28] Y. Shamir, Nucl. Phys. B **406**, 90 (1993).
 - [29] D. J. Antonio *et al.*, Phys. Rev. D **77**, 014509 (2008).
 - [30] O. Bar, C. Bernard, G. Rupak and N. Shoreh, Phys. Rev. D **72**, 054502 (2005).
 - [31] C. Aubin, J. Laiho and R. S. Van de Water, Phys. Rev. D **77**, 114501 (2008).
 - [32] J. -W. Chen, D. O'Connell, R. S. Van de Water and A. Walker-Loud, Phys. Rev. D **73**, 074510 (2006).
 - [33] B. C. Tiburzi, Phys. Rev. D **72**, 094501 (2005).
 - [34] C. Aubin, J. Laiho and R. S. Van de Water, Phys. Rev. D **75**, 034502 (2007).
 - [35] J. -W. Chen, D. O'Connell and A. Walker-Loud, Phys. Rev. D **75**, 054501 (2007).
 - [36] M. Golterman, T. Izubuchi and Y. Shamir, Phys. Rev. D **71**, 114508 (2005).
 - [37] D.B. Renner *et al.*, LHP Coll., Nucl. Phys. Proc. Suppl. **140** (2005) 255; R. G. Edwards *et al.*, PoS LAT **2005**, 056 (2006).
 - [38] Z. Fu, JHEP **1207**, 142 (2012); Z. Fu, JHEP **1201** (2012) 017; Z. Fu, Phys. Rev. D **85** (2012) 014506; Z. Fu, Phys. Rev. D **85** (2012) 074501; Z. Fu, Phys. Rev. D **87**, **074501** (2013); Z. Fu and K. Fu, Phys. Rev. D **86** (2012) 094507; Z. Fu, Commun. Theor. Phys. **57**, 78 (2012); Z. Fu, Eur. Phys. J. C **72**, 2159 (2012).